Modern Journal of Health and Applied Sciences *(MJHAS)*

E-ISSN 3078-2791; P-ISSN 3078-2783

Journal homepage: https://mucjournals.muc.edu.ps

Experimental and computational analysis of the corrosion inhibition performance of 2-[2-(hydroxy benzylidene)amino]benzoic acid Schiff base on mild steel in 1M hydrochloric acid

Zakariyya Danyaro[1*], *Rabiu Sabo*[2], *Ismail Alhassan*[3], *Nura Garba*[1], *and Abdulhamid Isah Lurwanu*[1]

[1]Department of Chemistry Jigawa State College of Remedial and Advanced Studies Babura Jigawa State Nigeria.
[2]Department of Chemistry, Sule Lamido University Kafin Hausa Jigawa State.
[3]Department of Chemistry Jigawa State College of education Gumel.

ARTICLE INFO

Received: 12th January 2025
Received in revised form: 08th February 2025
Accepted:10th February2025
Published: 15th March 2025

***Corresponding Author:**
Zakariyya Danyaro
E-mail:
zakariyyadanyaro@gmail.com

Citation: Danyaro, Z., Sabo, R., Alhassan, I., Garba, N., & Isah Lurwanu, A.(2025).Experimental and computational analysis of the corrosion inhibition performance of 2- [2-(hydroxy benzylidene) amino] benzoic acid Schiff base on mild steel in 1M hydrochloric acid. *Modern Journal of Health and Applied Sciences*, 2(1), 75-92.

DOI: https://doi.org/10.70411/MJHAS.2.1.2025195

ABSTRACT

The corrosion inhibition efficiency of 2-[2-(hydroxybenzylidene)amino] benzoic acid Schiff base on mild steel in an acidic medium was evaluated using gravimetric analysis and potentiodynamic polarisation (PDP) techniques. Characterization via FTIR and SEM confirmed the formation of a protective inhibitor layer on the metal surface. The inhibitor's efficiency increased with concentration, reaching 89.98% at 0.4 mM, but decreased with temperature, dropping to 51.54% at 333 K. PDP analysis classified the Schiff base as a mixed-type inhibitor, and the adsorption followed the Langmuir isotherm. A negative value of ΔG_{ads} (-34.04 kJ/mol) indicates strong and spontaneous adsorption. DFT calculations highlighted strong electron density around the C=N and hydroxyl groups, reinforcing the physisorption mechanism. Overall, experimental and computational results validated the Schiff base as an effective corrosion inhibitor for mild steel in 1 M HCl, demonstrating strong adsorption and excellent protective properties.

Keywords: Corrosion, Schiff base, PDP, SEM, DFT, and MDS.

1. Introduction

Corrosion poses a significant challenge for various industries, particularly for the common use of corrosion-sensitive mild steel under acid environments. Mild steel corrosion under hydrochloric acid solution is a significant challenge for petrochemical, building, and manufacturing industries where acid cleaning, pickling, and descaling operations are common. The corrosion inhibitors were studied extensively to address this challenge, and Schiff bases were identified as one promising organic inhibitor type (Chahul et al., 2015; Muhammad et al., 2024). Schiff bases, characterised by the azomethine (–C=N–), often exhibit limited solubility in aqueous acidic environments due to their molecular structure. However, the presence of functional groups such as hydroxyl (–OH) and carboxyl (–COOH) in 2-[2-(hydroxybenzylidene)amino]benzoic acid may enhance its solubility in acidic media through hydrogen bonding and protonation mechanisms. The solubility trend for structurally similar benzoic acid derivatives has also been extensively studied using various solvents, providing the basis for the understanding of the trend for this Schiff base (Kaabi et al., 2021; Ma et al., 2021). They are synthesized through the carbonyl compounds' condensation reaction with primary amines. They work by adsorbing onto the surface of the metal and forming protective layers over the surface, shielding against corrosive interactions. Having heteroatoms such as nitrogen, oxygen, and sulfur in their structure increases their electron-donating capacity, thus forming strong interactions against the surface of the metal (Ma'rufah et al., 2021). While the corrosion inhibition efficiency can be assessed by experimentations—i.e., chemical, electrochemical, and surface morphology analysis of the metals—a greater understanding about the mode of interaction between inhibitor molecules and the surface of the metal can be attained through the use of the computational calculations (Bouhraoua et al., 2023; Khamaysa et al., 2021; Khamaysa et al., 2020). DFT (density functional theory) modelling of inhibitor–metal interactions has emerged from recent studies as being very useful for the corrosion inhibition processes prediction. Considering the above points, this work investigates the corrosion inhibition efficiency and adsorptivity characteristics of the Schiff base 2-[2-(hydroxybenzylidene)amino] benzoic acid for the corrosion of mild steel under the impact of 1M HCl solution. Inhibition efficiency against corrosion was evaluated by weight loss measurements and potentiodynamic polarization analysis. Besides this, the surface morphology of the steel surface after corrosion exposure has also been studied by scanning electron microscopy (SEM). To complement the experiment data, detailed computer calculations were performed for the investigation of electronic and chemical reactivity features of the investigated inhibitors and their adsorptivity towards the steel surface. Results will yield valuable insights into its mode of inhibition, absorptivity features, and suitability towards industrial corrosion inhibition.

2. Methods and material

2. 1. Schiff base synthesis

Drop by drop, while stirring, 2-hydroxybenzaldehyde (6.08ml, 7.29mmol) was added to 50ml of hot absolute ethanol after 2-aminobenzoic acid (10.00g, 7.29 mmol) had been dissolved in 50 ml of hot ethanol. After refluxing for two hours, an orange precipitate formed overnight. The resulting solution was filtered, cleaned with cold ethanol, and allowed to air dry. The product was dried in a desiccator after being recrystallised from heated ethanol (I.A et al., 2020).

2. 2. Specimen preparation

Mild steel was the specimen (coupons) used in this study. C 0.21%, Si 0.38%, P 0.1%, S 0.04%, Mn 0.05%, and Al 0.01% make up the mild steel's chemical composition, with Fe making up the remaining portion. The mild steel was cut into dimensions of 4 cm by 2.5 cm by 0.1 cm. It underwent chemical treatments, including acetone drying and absolute ethanol degreasing (Selatnia et al., 2018). Before the experiment, the coupons were placed in desiccators. All the chemicals used here are analytical grades .

2. 3. Weight loss measurement

The experiment involved weighing coupons, submerging them in a 1M HCl solution with or without inhibitor concentrations, covering them with aluminum foil, and placing them in a water bath at 30°C for various time periods. The weight loss, corrosion rate, inhibition efficiency, and surface coverage were determined using equations (Benahmed et al., 2020):

$$\text{Weight loss } (\Delta W) = W_2 - W_1 \quad (1)$$

$$C_R \text{ (mg/cm}^2\text{h)} = \frac{\Delta W(mg)}{A(sq.cm) \times T(h)} \quad (2)$$

$$\text{I.E \%} = \left(1 - \frac{W1}{W2}\right) \times 100 \quad (3)$$

$$\Theta = 1 - \frac{W1}{W2} \quad (4)$$

Where C_R is the corrosion rate, A is the mild steel coupon's area (cm^2), I.E. is the inhibition efficiency, t is the immersion duration (in hours), Θ is the surface coverage, and W1 and W2 are the weight losses for the mild steel coupon with and without inhibitor, respectively (Jimoh & Musa, 2024).

2. 4. Analyses of Potentiodynamic Polarisation (PDP)

The study investigates the corrosion rate of mild steel coupons by immersing them in a 1M HCl solution containing inhibitors at different concentrations. The coupons were analyzed using Autolab potentiostat and NOVA software, with the results depicted in a graph of potential versus current density. The inhibitory efficiency was computed using Equation 5, which includes the corrosion potential and current density. The experiment aimed to understand the effects of different inhibitors on corrosion.

$$\%I = \frac{I\,corr\,(0) - Icorr(inh)}{Icorr(0)} \times 100 \quad (5)$$

Where $I_{corr}(inh)$ and $I_{corr}(0)$ are the corrosion current densities with and without the inhibitor (Khan et al., 2017).

2. 5. Fourier Transform Infra-Red Spectrophotometry (FT-IR)

FT-IR spectra were used to analyse the corrosion products and Schiff base. For four days, coupons were submerged in HCl to form an adsorbed layer. They were scanned for analysis after drying. The surface morphologies of mild steel were investigated using SEM. Prior to examination, the samples were dried after being immersed in HCl for a whole day (Shkoor et al., 2023).

2. 6. Research on computations

Quantum chemistry simulations were conducted using Density Functional Theory (DFT) Gaussian 09 software, optimizing the inhibitor structure in the gas phase. The ionisation potential and electron affinity were calculated using Koopman's theorem.

$$I = -E_{HOMO} \quad (6)$$

$$A = -E_{LUMO} \quad (7)$$

The electronegativity (ƛ), softness (σ) and hardness (η) were determined using **equations (8 – 10)** respectively.

$$ƛ = \frac{I+A}{2} \quad (8)$$

$$\eta = \frac{I-A}{2} \quad (9)$$

$$\sigma = \eta^{-} \quad (10)$$

The fractional number of transferred electrons (ΔN) was determined using equation 11.

$$\Delta N = \frac{\lambda Fe - \lambda inh}{2(\eta Fe + \eta inh)} \quad (11)$$

For iron (λFe), the electronegativity value was 7ev, and as per equation 12, the hardness of iron (ηFe) was 0eV.

$$\Delta N = \frac{7 - \lambda inh}{2(\eta inh)} \quad (12)$$

The difference between the electrophilic and nucleophilic Fukui functions is what is defined as the second Fukui function, or dual description, in equation (13- 15). Where f^2 (r) is less than zero, site K promotes an electrophilic attack. This implies that f^2 (r) serves as a selectivity index for attacks that are either nucleophilic or electrophilic .

$$F(k)^+(\text{nucleophilic attack}) = qk(N+1) - qk(N) \quad (13)$$

$$F(k)^-(\text{electrophilic attack}) = qk(N - qk(N-1) \quad (14)$$

$$F(r) = f^- - f^- = f^2 \text{ (Fukui function)} \quad (15)$$

2. 7. Molecular dynamics simulation

The study used COMPASS FORCEFIELD and smart ALGORITH to simulate the surface of iron. The fractional depth of 3.0 was used to separate Fe crystals along the Fe (111) plane. The iron surface was developed into a 10 x 10 supercell to minimize edge effects. The temperature was set at 350K to quench molecules on the surface. Different interactions were produced, and binding energy between inhibitors and the Fe (111) surface was calculated (Awe et al., 2015)

$$\text{Binding energy} = E_{total} - (E_{inhibitor} + E_{Fe\ surface}) \quad (16)$$

3. Result and discussion

3. 1. Effect of Time on Corrosion

Experimental analysis was used to study the effect of time on the corrosion control of mild steel using the Schiff base. The study was carried out at a constant temperature (303K) at varying concentrations of the Schiff base (0.1 to 0.4mM), and time (1 h to 4 h).

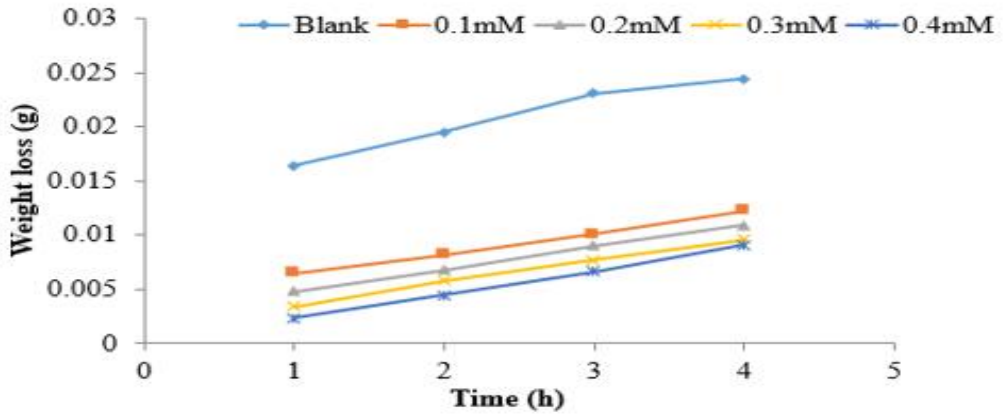

Figure 1. Variation of Weight loss (g) with time (h) for the corrosion of mild steel in 1.0M HCl in the absence and presence of different concentration of Schiff base at 303K

Weight loss rose as immersion duration increased, as seen in the **Figures 1**. According to the result, mild steel loses less weight when an inhibitor is present than when it is not. The reduction in weight loss was caused by the Schiff base adsorption on the metal surface. Different researchers came up with similar conclusions (Ameh & Eddy, 2018; Husaini et al., 2018)

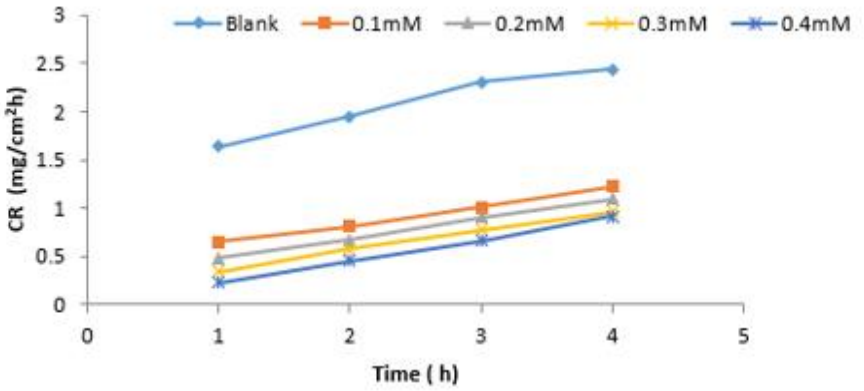

Figure 2. Effect of immersion time on the corrosion rates of mild steel in 1.0 M HCl in the absence and presence of Schiff base

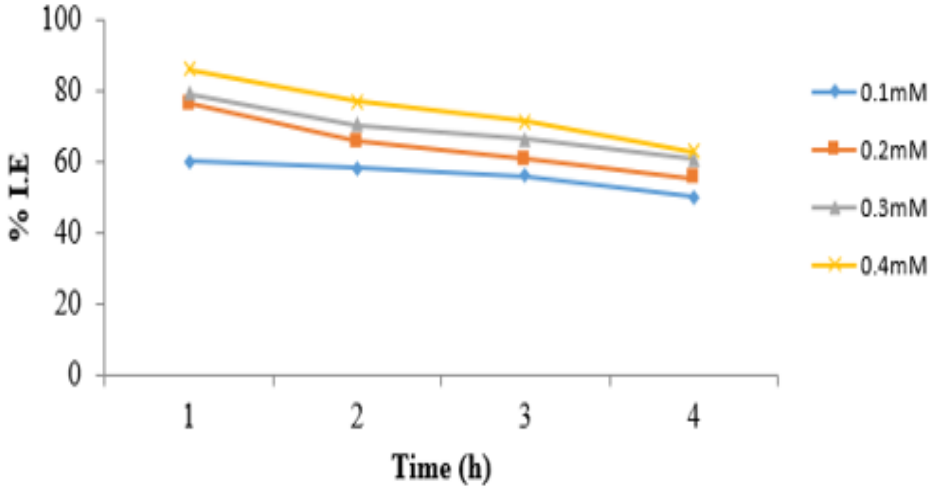

Figure 3. Effect of Immersion Time (h) on Corrosion Inhibition Efficiency (%IE) of mild steel in 1.0 M HCl in the presence of various concentrations of Schiff base

Figures 2 and **3** illustrate the corrosion rate and inhibition efficiency of mild steel in 1.0 M HCl 303K as a function of time in the presence of Schiff bases, respectively, using the weight loss technique. **Figure 2** makes it clear that as the inhibitor concentration increased, the mild steel coupons' corrosion rates in the presence of Schiff base reduced. In the meanwhile, **Figure 3** makes it evident that as immersion duration grew, inhibition efficiency declined. This outcome is consistent with what Musa et al. (2018), Chahul et al.,(2019), Sefiyyah & Magaji, (2023) reported (Chahul et al., 2019; Husaini et al., 2018; Minjibir & Ladan, 2023).

3. 2. Effect of Temperature

The effect of temperature on the weight loss of mild steel in the absence and presence of Schiff base in a 1M HCl solution is shown in **Figures 4.**

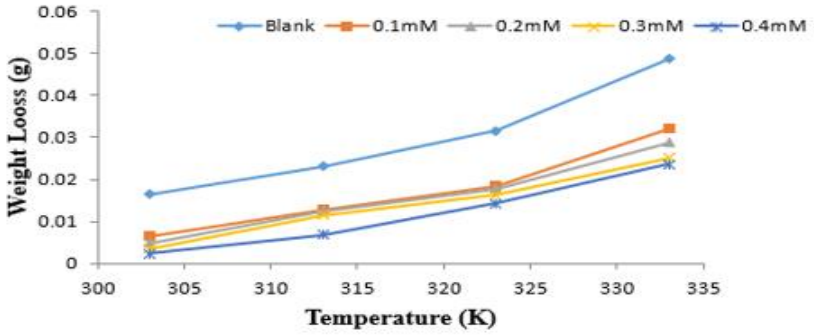

Figure 4. Variation of weight loss with temperature for the corrosion of mild steel in absence and presence of Schiff base in 1M HCL

Table 1. Weight loss, corrosion rate, surface coverage inhibition efficiency of various concentration of Schiff base in 1M HCl at varying temperature.

Temperature (K)	Concentration (mM)	ΔW (g)	CR (mg/cm²h)	Θ	% I.E
303	Blank	0.0164	1.64	-	-
	0.1	0.0065	0.65	0.6036	60.36
	0.2	0.0048	0.48	0.7073	70.73
	0.3	0.0034	0.34	0.7927	79.27
	0.4	0.0023	0.23	0.8998	89.98
313	Blank	0.0231	2.31	-	-
	0.1	0.0128	1.28	0.4459	44.59
	0.2	0.0125	1.25	0.4589	45.89
	0.3	0.0115	1.15	0.5022	50.22
	0.4	0.0068	0.68	0.7056	70.56
323	Blank	0.0315	3.15	-	-
	0.1	0.0184	1.84	0.4159	41.59
	0.2	0.0178	1.78	0.4349	43.49
	0.3	0.0162	1.62	0.4857	48.57
	0.4	0.0142	1.42	0.5492	54.92
333	Blank	0.0487	4.87	-	-
	0.1	0.0320	3.20	0.3429	34.29
	0.2	0.0288	2.88	0.4086	40.86
	0.3	0.0251	2.51	0.4846	48.46
	0.4	0.0236	2.36	0.5154	51.54

The kinetic energy of the reaction increased as temperature rose, accelerating corrosion. However, as the Schiff base concentration increased, the weight loss decreased. **Table 1** and **Figure 4** show that the corrosion rate increases as temperature rises, but inhibition effectiveness decreases. This suggests that the Schiff base slows mild steel dissolution, but the rate of

chemical reaction also increases, causing the surface to etch and desorb more quickly (Abbas et al., 2018; Ameh & Eddy, 2018; Eddy et al., 2015; Godwin-Nwakwasi et al., 2017).

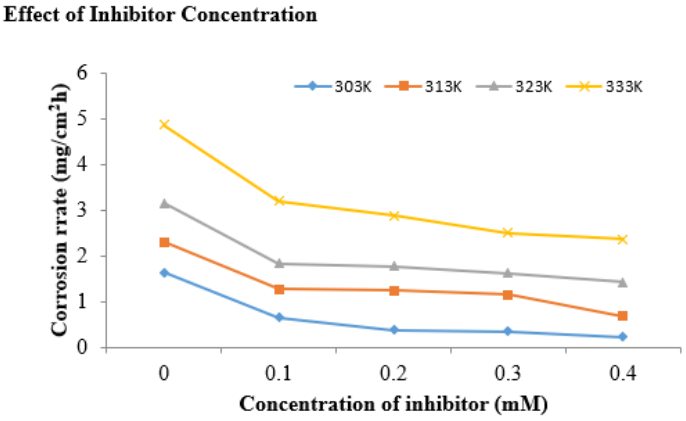

Figure 5. Variation of Corrosion Rate with Inhibitor Concentration of Schiff base for mild steel corrosion in HCl

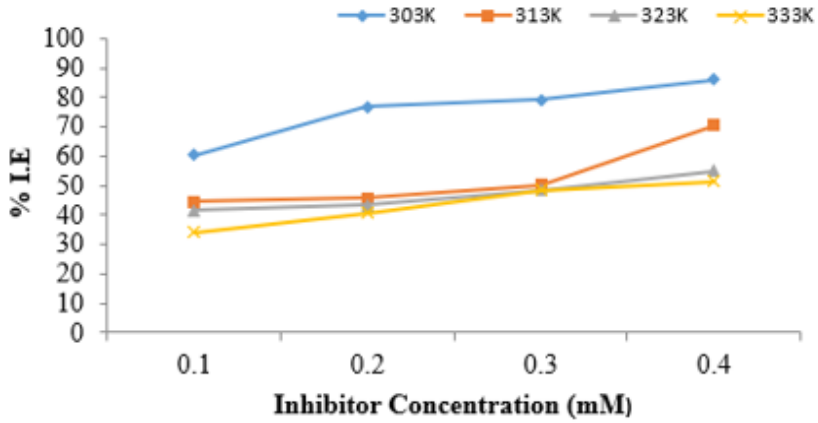

Figure 6. Variation of Inhibition Efficiency with Inhibitor Concentration of Schiff base for Mild steel Corrosion in HCl

The study demonstrates that inhibited systems have a lower corrosion rate than uninhibited ones in 1M HCl. The corrosion rate decreases with increasing inhibitor concentration as inhibitor molecules are adsorbed on the surface, creating a barrier that slows down the corrosion process. The inhibitor's effectiveness increases with concentration, as mild steel absorbs more of the inhibitor's molecules at higher concentrations. The adsorption isotherm, based on surface coverage, was used to understand the interaction between the inhibitor and the mild steel surface. The Langmuir adsorption isotherm was found to be the best fit for the data (Asmara et al., 2018; Chahul et al., 2015; Yaro et al., 2013).

$$\frac{Cinh}{\theta} = \frac{1}{Kads} + C_{inh} \qquad (17)$$

Where K_{ads} is the adsorption equilibrium constant, surface coverage (Θ) and Cinh is the concentration of inhibitor. A graph of $\frac{Cinh}{\theta}$ against Cinh was plotted as shown in **Figure 7.**

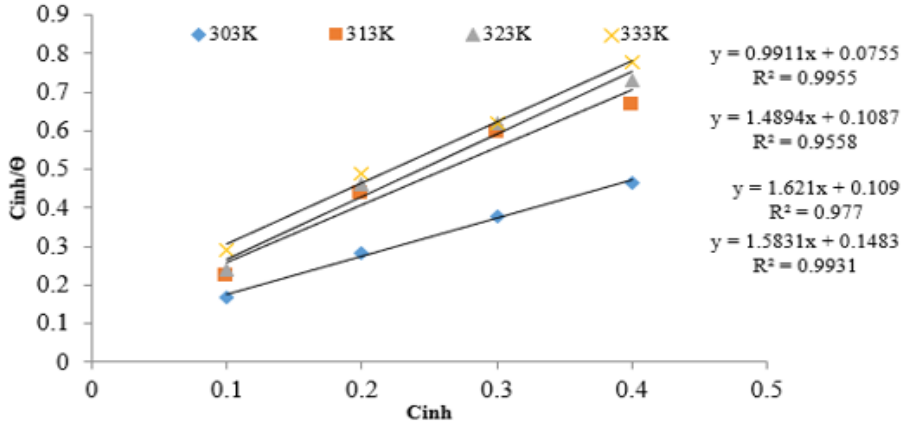

Figure 7. Langmuir adsorption plots for the corrosion of mild steel in IM HCl solution in the presence of the SB1 at different temperature

Table 2. Adsorption parameters for the adsorption of Schiff base on mild steel surface

Isotherm	Temperature (K)	Slope	K_{ads} x10^3	ΔG_{ads} (kJ/mol)	R^2 values
Langmuir	303	0.991	13.333	-34.045	0.995
	313	1.489	9.259	-34.222	0.955
	323	1.489	9.174	-35.291	0.977
	333	1.583	6.757	-35.537	0.993
Freundlich	303	0.254	1.086	-27.731	0.952
	313	0.281	0.794	-27.830	0.641
	323	0.191	0.625	-28.078	0.855
	333	0.303	0.684	-29.195	0.987
Temkin	303	0.183	1.017	-27.565	0.988
	313	0.156	0.763	-27.727	0.606
	323	0.090	0.608	-28.003	0.833
	333	0.127	0.630	-28.968	0.979

The Langmuir adsorption isotherm plots show that Schiff bases adsorb at temperatures between 30 and 60 degrees Celsius, with frequent sites at the metal/solution interface. The adsorption equilibrium constant (K_{ads}) decreases as temperature rises, suggesting stronger engagement between inhibitor molecules and mild steel. At 303 K, the adsorption equilibrium constant (K_{ads}) value is greater, suggesting Schiff base is more effective as an inhibitor (Aljibori et al., 2024; Koraee et al., 2019; Siaka et al., 2013).

3. 3. Free energy of Adsorption

Equations 18(a, b) relate the adsorption equilibrium constant (K_{ads}) to the adsorption free energy (ΔG_{ads}).

$$K_{ads} = \frac{1}{55}\exp\left(\frac{-\Delta Gads}{RT}\right) \quad (18a)$$

This can be written as:

$$\Delta G_{ads} = -RT \ln (55.5K_{ads}) \quad (18b)$$

The study investigates the adsorption of Schiff base on mild steel using a combination of chemisorption and physisorption modes. The adsorption rates at different temperatures were used to calculate the activation energy of mild steel coupon corrosion in 1.0 M HCl with and without Schiff base. The results show that inhibitor molecules adsorb spontaneously on the mild steel surface, while the Langmuir isotherm shows a combination of chemisorption and physisorption modes (Ameh et al., 2012; Olasehinde et al., 2012; Omotosho, 2016).

$$ln(CR) = A - \frac{Ea}{RT} \quad (19)$$

Where A is the Arrhenius pre-exponential factor, C_R is the rate of corrosion, T is the absolute temperature in Kelvin and R is the universal gas constant.

Table 3. Energy parameters for the dissolution of Mild Steel in IMCI in the absence and presence of difference concentration of Schiff base

Concentration (mM)	E_a (kJ/mol)	ΔH (kJ/mol)	ΔS (kJ/mol)
Blank	29.723	27.11	-0.152
0.1	42.768	40.14	-0.116
0.2	47.607	45.03	-0.101
0.3	52.712	50.05	-0.087
0.4	64.193	61.58	-0.053

The activation energy (E_a) of a Schiff base in mild steel was found to slow corrosion in 1.0M HCl, possibly due to its uniform adsorption on the metal's surface. The study found that chemisorption requires an activation energy of 80 kJ/mol or higher, while physisorption requires less than 80 kJ/mol (Jeyaprabha & Bhuvaneswari, 2020). The study also used the transition state equation to calculate the enthalpy and entropy of activation.

$$\ln \frac{CR}{T} = [\ln (\frac{R}{hN}) + (\frac{\Delta S*}{R})] - \frac{\Delta H*}{RT} \quad (20)$$

The study reveals that the mild steel dissolution process is endothermic, with adsorption heat increasing with increasing inhibitor concentration. The activation values' entropy changes decrease as the inhibitor concentration rises, suggesting a reduction in disorder as it moves from the reactant to the activated complex. The study also introduces potentiodynamic polarization for inhibited and uninhibited corrosion for the corrosion system of the mild steel, and the electrochemical characteristics for corrosion for the corrosion of the mild steel metal under various Schiff base concentrations in the 1M HCl solution (Gaya et al., 2019; Jeyaprabha & Bhuvaneswari, 2020).

3. 4. Potentiodynamic polarization

Figure 8. Is the potentiodynamic polarization curve for the inhibited and uninhibited corrosion system for the mild steel and the table for the electrochemical parameters for the corrosion of the mild steel metal in the solution containing 1M HCl and various Schiff base concentrations from the Tafel curve is provided in Table 4.

Table 4: Electrochemical characteristics for mild steel metal corrosion in 1M HCl solution with varying concentrations of Schiff base

Inhibitor Conc (mM)	I_{Corr} ($mAcm^{-2}$)	E_{Corr} (mV)	B_a ($mVdec^{-1}$)	B_C ($mVdec^{-1}$)	C. R D ($mmpy^{-1}$)	% I.E
0.0	8.63	-565.97	185.70	460.47	4.77	-
0.1	6.16	-569.62	168.10	371.10	3.41	28.58
0.2	2.85	-558.53	112.80	209.60	1.58	66.92
0.3	2.21	-566.92	98.90	130.40	1.22	74.38
0.4	1.82	-563.31	65.60	105.90	1.01	78.86

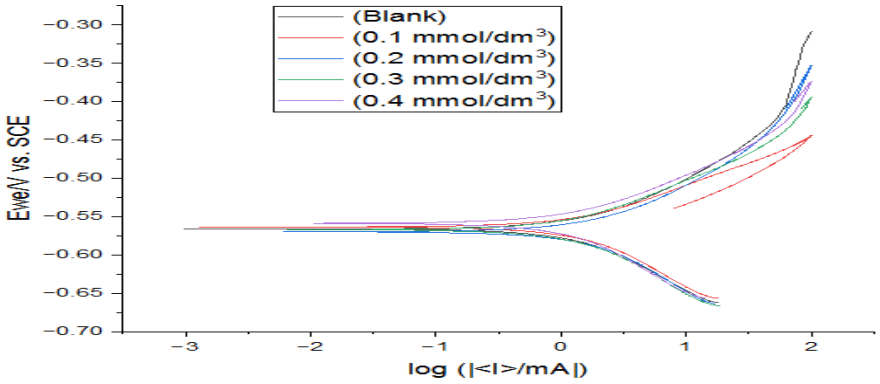

Figure 8. Tafel plot of the mild steel in the absence and presence of Schiff base

The study examined the effects of Schiff bases on anodic and cathodic plots on a mild steel electrode in a 1M HCl. The results showed that the addition of Schiff bases affected the anodic and cathodic parts of the Tafel slopes. The addition of an inhibitor molecule to an acidic medium reduced the formation of hydrogen gas and anodic metal dissolution, suggesting that inhibitor concentrations affected both reactions (Oshomogho et al., 2020; Pankaj & Gargi, 2014; Ravari & Dadgarinezhad, 2012).

3. 5. Surface morphology

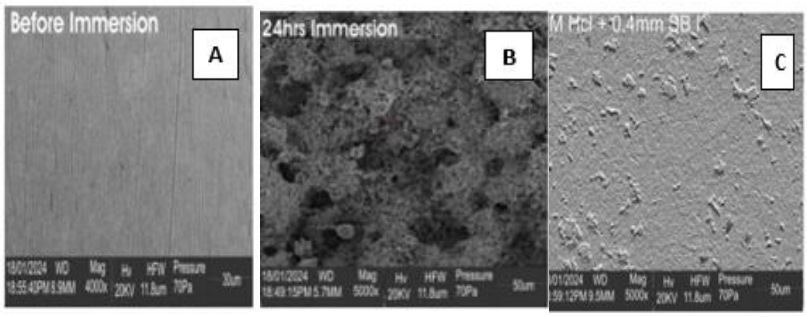

Figure 9. SEM micrographs of mild steel surface after immersion in IM HCl for 24 hours at room temperature: (a) Polished Mild Steel surface; (b) Mild steel immersed in 1M HCl (c) immersion in 1M HCl containing 0.4mM SB inhibitor

SEM imaging was used to analyze the shape of a mild steel surface. Results showed pitting and cracking in the absence of inhibitors, while a smooth surface was observed when inhibitors were present. This suggests that mild steel cannot dissolve when a Schiff base inhibitor is present, as it creates a protective coating (Ijuo et al., 2016; Musa et al., 2020).

3. 6. Fourier Transform Infra-Red Spectroscopy

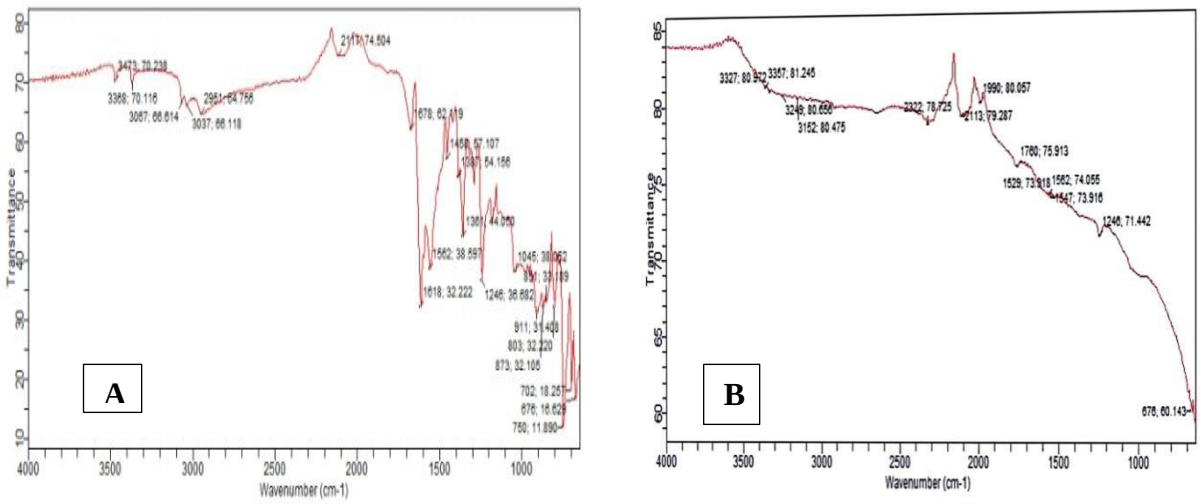

Figure 10. FTIR spectrum of (A) Schiff base (b) Corrosion product of mild steel in 1M HCl medium with 0.3mM SB

FTIR spectroscopy confirmed the inhibitor's adsorption behavior on mild steel surfaces. The inhibitor's FTIR spectrum showed frequency shifts, suggesting interaction with SB and SB2. The mild steel surface interacts with SB and SB2, resulting in SB adsorbed using a pi-electron and a functional group (Alian & Andresman, 2017; Eddy et al., 2011; Verma & Khan, 2016).

3. 7. Quantum Chemical Parameters

With the density, highest occupied molecular orbital (HOMO), lowest unoccupied molecular orbital (LUMO), and optimal structure, the structure in **Figures 11.** Depicts the optimal molecules of Schiff base.

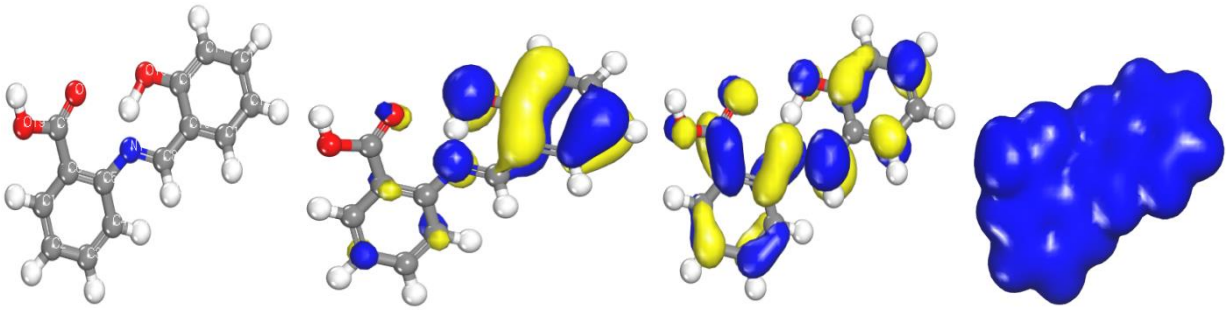

Optimized molecules HOMO LUMO Density

Figure 11. Showing the optimized structure, HOMO orbital, LUMO orbital and Density of the molecule.

Table 5. The chemical parameters of Schiff bases at the DFT/B3LYPB/6-3IG (d) theory level

Properties	SB
E_{HOMO}	-5.331

E_{LUMO}	-3.050
Energy gap (eV)ΔE	2.281
Ionization energy (eV)I	5.331
electron affinity (eV) A	3.050
Absolute electronegativity (eV)χ	4.191
Global hardness (eV)η	1.141
Global softness (eV) $^{-1}$σ	0.876
ΔN (Fraction of electron transferred)	1.231
Global electrophilicity index (eV)ω	7.695
Nucleophility (eV) Ɛ	0.130
Back donation(eV)ΔE_{b-d}	-0.285

Researchers used the frontier molecular orbital (FMO) concept to study the reactivity and interaction between an inhibitor molecule and a mild steel surface (Ishaq & Ladan, 2023). The Schiff base molecules showed a strong ability to donate and receive electrons from the metal and mild steel, with lower E_{LUMO} values indicating a greater electron donation tendency. The Schiff base molecule's value for E_{HOMO} being 5.331 eV suggests that the corrosion impact can be reduced by the Schiff base molecule (Nyijime et al., 2023). ΔE ($E_{LUMO} - E_{HOMO}$) also played its part towards the efficiency of the barrier being one that is active towards corrosion (Shehu & Usman, 2023). The Schiff base molecule's lower value for the ionisation energy suggests its flexibility. Acid-base hypothesis suggests the softer the molecule is, the greater will the level of the inhibitor effectiveness will be. Inhibitory effectiveness for the Schiff base containing greater global softness has also been said to be greater. Interaction for the inhibitory molecule towards the surface of the metal has also been proved using the reverse donation ΔE_{b-d} energy (Esan et al., 2022; Siaka et al., 2014).

\

Table 6. Fukui functions of the molecule used for the inhibition

Atom of SB1	Fukui(+) Nucleophilic attack	Fukui (-) Electrophilic attack	f^2
C (1)	0.03	0.016	0.014
C (2)	0.043	0.025	0.018
C (3)	0.038	0.017	0.021
C (4)	0.028	0.022	0.006
C (5)	0.032	0.014	0.018
C (6)	0.036	0.017	0.019
N (7)	0.033	0.062	-0.029
C (8)	**0.094**	0.041	0.053
H (9)	0.033	0.025	0.008
C (10)	0.027	0.057	-0.03
C (11)	0.044	0.057	-0.013
C (12)	0.034	0.104	-0.07
C (13)	0.054	0.046	0.008
C (14)	0.034	0.078	-0.044
C (15)	0.041	0.059	-0.018
O (16)	0.073	**0.121**	-0.048
C (17)	0.048	0.011	0.037
O (18)	0.053	0.02	0.033
O (19)	0.04	0.009	0.031
H (20)	0.018	0.007	0.011

H (21)	0.019	0.011	0.008
H (22)	0.018	0.009	0.009
H (23)	0.016	0.012	0.004
H (24)	0.021	0.03	-0.009
H (25)	0.018	0.039	-0.021
H (26)	0.022	0.027	-0.005
H (27)	0.019	0.035	-0.016
H (28)	0.013	0.023	-0.01
H (29)	0.02	0.003	0.017

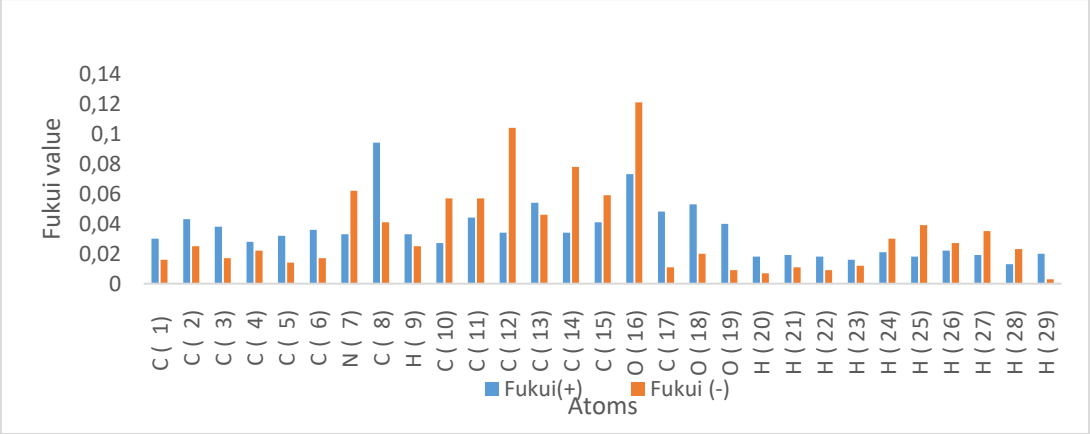

Figure 12. Fukui in graphical representation

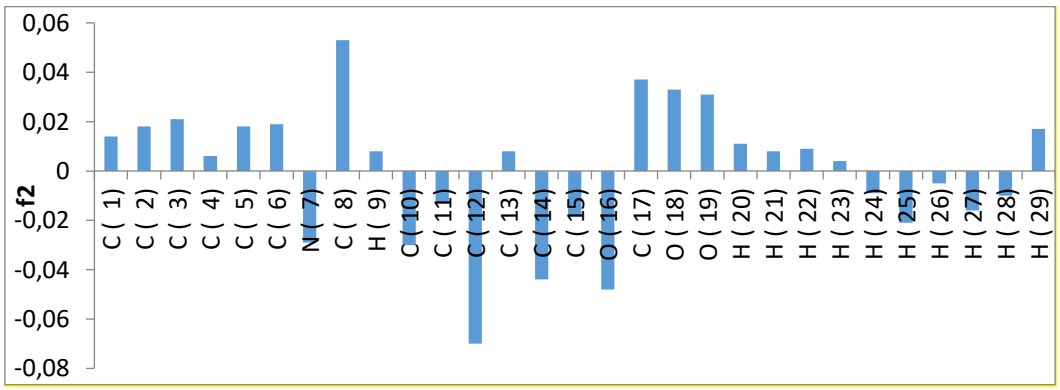

Figure 13. Second function

Table 7. Percentage of second order Fukui function

Inhibitor	Nucleophile	Electrophile
SB1	58.62%	41.38%

The study investigates the inhibitor molecules' reactivity over the surface of the metal using the Fukui indices, which define the molecules' parts responsible for nucleophilic and electrophilic attacks. Limited acceptor-donor interaction is responsible for the inhibitor molecules' reactivity over the surface of the metal. In the study, the highest f+ value atoms were the best sites for nucleophilic and electrophilic attacks when the highest value for the Fukui function is attained. Schiff base, being nucleophilic, is the best inhibitor for corrosion prevention over the surface of the metal for the case of iron. Molecular dynamic simulation data indicate the compounds under investigation adsorbed over the surface, where adsorption and the type of the energy for the

binding were calculated using the Forcite quench dynamic simulation technique. According to the molecular dynamic simulation data, the compounds under investigation adsorbed over the surface .

3. 8. Molecular dynamic simulation

The Forcite quench dynamic simulation method has been applied for the estimation of adsorption and the energy of binding.

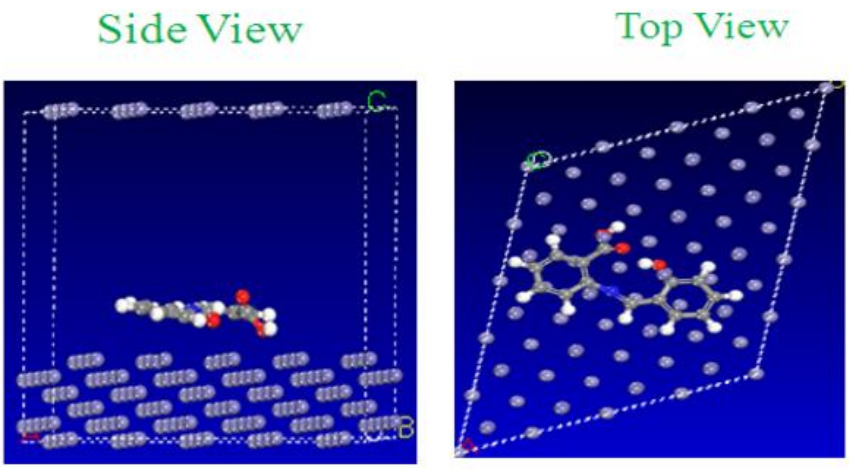

Figure 14. The snapshots (side view and top view) of the simulation as the optimized molecules interact with the Fe (111) surface

Table 8. Interaction energies of the Schiff bases molecules on Fe (111) simulation

Properties	Properties
Energy of the Fe (111) (kcalmol^{-1})	0.0000±0.0
Adsorption Energy (kcalmol^{-1})	-98.180±0.3
Binding Energy (kcalmol^{-1})	98.180±0.3

Molecular dynamic simulations were carried out for the evaluation of the adsorption of the inhibitor onto the surface of the metal at the molecular level. Forcite quench was used for the sampling of different low-energy structures and the discovery of the low-energy minima (Siaka et al., 2014) Mild steel adsorption by the inhibitor molecules reported were simulated by the modelling of the interactions of the inhibitor molecules and the surface of the Fe (111) crystal.

Equations 21 and 22 were used to determine the adsorption energy and binding energy for the interaction between the Schiff bases and the surface of Fe (111).

$$E_{ads} = E_{total} - (E_{mol} + E_{Fe}) \quad (21)$$

$$E_{binding} = - E_{ads} \quad (22)$$

Where E_{mol}, E_{Fe} and E_{total} are the total energies of the molecules, Fe (111) and the adsorbed Mol/Fe (111) coupled in the gas phase respectively.

The study focuses on the adsorption and inhibition potential of inhibitor molecules on the metallic surface of Fe (111) using simulated systems. The binding and adsorption energies on the metal surface are crucial for evaluating inhibitory effects. The results align with experimental values, with adsorption energies less than 100 kcal/mol, which are within the range of physisorption interactions. The adsorption energy of the inhibitor-metal interface is inversely related to the inhibitor's degree of adsorption onto the metal surface.

4. Conclusion

The research leads to the following conclusion:

- The synthesis of the Schiff base was accomplished effectively.
- In a 1M HCl solution, the Schiff base effectively inhibits mild steel corrosion, exhibiting an inhibition effectiveness of 89.98% at a concentration of 0.4mM. The corrosion efficiency rose as the concentration of the inhibitor increased and fell as the temperature rose.
- The inhibitor functions as a mixed-type inhibitor, according to polarisation studies.
- The Langmuir adsorption isotherm is followed by the adsorption of Schiff bases on the surface of mild steel in a 1M HCl solution, which is categorised as chemical adsorption. The endothermic character of the process was shown by the positive enthalpy change of activation (ΔHad) in both blank and inhibited acid solutions. The process was entropically favorable, as shown by the negative activation entropy (ΔSad). Additionally, the spontaneity of the adsorption process was demonstrated by the negative values of ΔGads.
- The FTIR showed that the inhibition is caused by the adsorption of certain functional groups and aromatic rings in the Schiff bases, while the SEM result showed that the mild steel surface is shielded by adsorption coatings.
- The Schiff bases were adsorbed on the mild steel surface by a physisorption process, with inhibitory efficacy based on molecule size, according to the quantum chemical calculation.
- The information gathered using a range of techniques (both experimental and theoretical) shows a strong correlation, indicating the reliability and quality of the data. The metal surface is in closer contact with the Schiff base due to electron donation and acceptance, which results in lower energy levels. The quantum computation verified the Schiff base's high inhibitory efficiency.

Conflict of Interest

On behalf of all authors, the corresponding author states that there is no conflict of interest.

Data Availability

No data was used for the research described in the article

Reference

Abbas, A., Fazakas, É., & Török, T. (2018). Corrosion studies of steel rebar samples in neutral sodium chloride solution also in the presence of a bio-based (green) inhibitor. *International Journal of corrosion and scale inhibition*, *7*(1), 38-47.

Alian, H., & Andresman, Y. (2017). Analysis Of Corrosion Rate For Steel Concrete Reinforcing Pda Reinforced Concrete In Sea Water Media. *Journal of Mechanical Science and Engineering*, *4*(1), 017-022.

Aljibori, H. S., Alamiery, A., Gaaz, T. S., & Al-Azzawi, W. K. (2024). Exploring corrosion protection for mild steel in HCl solution: An experimental and theoretical analysis of an antipyrine derivative as an anticorrosion agent. *Carbon Neutralization*, *3*(1), 74-93.

Ameh, P. O., & Eddy, N. O. (2018). Theoretical and experimental investigations of the corrosion inhibition action of Piliostigma thonningii extract on mild steel in acidic medium. *Communication in Physical Sciences*, *3*(1).

Ameh, P. O., Magaji, L., & Salihu, T. (2012). Corrosion inhibition and adsorption behaviour for mild steel by Ficus glumosa gum in H2SO4 solution. *African Journal of Pure and Applied Chemistry*, *6*(7), 100-106.

Asmara, Y. P., Kurniawan, T., Sutjipto, A. G. E., & Jafar, J. (2018). Application of plants extracts as green corrosion inhibitors for steel in concrete-A review. *Indonesian Journal of Science and Technology*, *3*(2), 158-170.

Awe, F., Idris, S., Abdulwahab, M., & Oguzie, E. (2015). Theoretical and experimental inhibitive properties of mild steel in HCl by ethanolic extract of Boscia senegalensis. *Cogent Chemistry*, *1*(1), 1112676.

Benahmed, M., Selatnia, I., Djeddi, N., Akkal, S., & Laouer, H. (2020). Adsorption and corrosion inhibition properties of butanolic extract of Elaeoselinum thapsioides and its synergistic effect with Reutera lutea (Desf.) Maires (Apiaceae) on A283 carbon steel in hydrochloric acid solution. *Chemistry Africa*, *3*, 251-261.

Bouhraoua, A., Khamaysa, O., Selatnia, I., Lgaz, H., Sid, A., Zeghache, H., Ebenso, E. E., & Lee, H.-S. (2023). Experimental and computational studies on the corrosion mitigation properties of a newly synthesized imine derivative for carbon steel in HCl medium. *Journal of Molecular Structure*, *1284*, 135317.

Chahul, H., Ayuba, A., & Nyior, S. (2015). Adsorptive, Kinetic, Thermodynamic and Inhibitive Properties of Cissus Populnea Stem Extract on the Corrosion of Aluminum in Acid Medium. *ChemSearch Journal*, *6*(1), 20-30.

Chahul, H., Danat, B., & Maji, E. (2019). Corrosion inhibition performance of ethanol extract leaves of Cucurbita pepo (Pumpkin) on mild steel in acidic media. *ChemSearch Journal*, *10*(1), 46-53.

Eddy, N. O., Awe, F. E., Siaka, A. A., Magaji, L., & Ebenso, E. E. (2011). Chemical information from GC-MS studies of ethanol extract of Andrographis paniculata and their corrosion inhibition potentials on mild steel in HCl solution. *International Journal of Electrochemical Science*, *6*(9), 4316-4328.

Eddy, N. O., Momoh-Yahaya, H., & Oguzie, E. E. (2015). Theoretical and experimental studies on the corrosion inhibition potentials of some purines for aluminum in 0.1 M HCl. *Journal of advanced research*, *6*(2), 203-217.

Esan, T., Oyeneyin, O., Olanipekun, A., & Ipinloju, N. (2022). Corrosion inhibitive potentials of some amino acid derivatives of 1, 4-naphthoquinone–DFT calculations. *Adv. J. Chem.-Sect. A*, *5*, 263.

Gaya, H., Shawai, S., Yusuf, G., & Abubakar, I. (2019). Plants extract for corrosion control of mild steel in acidic medium. *World Academics Journal of Engineering Sciences*, *6*(1), 47-51.

Godwin-Nwakwasi, E. U., Elachi, E. E., Ezeokonkwo, M. A., & Onwuchuruba, L. E. (2017). A study of the corrosion inhibition of mild steel in 0.5 M tetraoxosulphate (VI) acid by Alstonia boonei leaves extract as an inhibitor at different temperatures. *International Journal of Advanced Engineering, Management and Science*, *3*(12), 1150-1157.

Husaini, M., Usman, B., & Ibrahim, M. B. (2018). Evaluation of corrosion behaviour of aluminum in different environment. *Bayero Journal of Pure and Applied Sciences*, *11*(1), 88-92.

I.A, I., S.D, M., S, S., & Almustapha, M. N. (2020). Synthesis of schiff base derived from anthranilic acid and its potentials on oil and gas pipeline corrosion inhibition. *Nigerian Research Journal of Chemical Sciences*, *8*(2), 57-68.

Ijuo, G., Chahul, H., & Eneji, I. (2016). Corrosion inhibition and adsorption behaviour of Lonchocarpus laxiflorus extract on mild steel in hydrochloric acid. *Ew. J. Chem. Kine*, *1*, 21-30.

Ishaq, N., & Ladan, M. (2023). Triazole Derivatives as Corrosion Inhibitors on Iron (110) Surface: A Theoretical Study. *ChemSearch Journal*, *14*(1), 54–65-54–65.

Jeyaprabha, C., & Bhuvaneswari, T. (2020). Thermodynamics, Adsorption and Spectral Studies of the Corrosion Inhibition of Mild Steel by Different Leaf Extracts in 1.0 N HCl: Comparative Analysis.

Jimoh, I., & Musa, L. (2024). EVALUATION OF THE CORROSION INHIBITION PROPERTIES OF ETHANOLIC EXTRACT FROM ACACIA NILOTICA POD ON MILD STEEL IN 0.1 M SULFURIC ACID: AN EXPERIMENTAL STUDY UTILIZING FTIR AND SEM TECHNIQUES.

Kaabi, I., Douadi, T., Daoud, D., Amamra, S., & Chafaa, S. (2021). A new synthesized schiff base as corrosion inhibitor for mild steel in a HCl medium: experimental, density functional theory and molecular dynamics simulation studies. *Port Electrochim Acta*, *39*(5), 349-379.

Khamaysa, O. M. A., Selatnia, I., Lgaz, H., Sid, A., Lee, H.-S., Zeghache, H., Benahmed, M., Ali, I. H., & Mosset, P. (2021). Hydrazone-based green corrosion inhibitors for API grade carbon steel in HCl: Insights from electrochemical, XPS, and computational studies. *Colloids and Surfaces A: Physicochemical and Engineering Aspects*, *626*, 127047.

Khamaysa, O. M. A., Selatnia, I., Zeghache, H., Lgaz, H., Sid, A., Chung, I.-M., Benahmed, M., Gherraf, N., & Mosset, P. (2020). Enhanced corrosion inhibition of carbon steel in HCl solution by a newly synthesized hydrazone derivative: Mechanism exploration from electrochemical, XPS, and computational studies. *Journal of Molecular Liquids*, *315*, 113805.

Khan, G., Basirun, W. J., Kazi, S. N., Ahmed, P., Magaji, L., Ahmed, S. M., Khan, G. M., Rehman, M. A., & Badry, A. B. B. M. (2017). Electrochemical investigation on the corrosion inhibition of mild steel by Quinazoline Schiff base compounds in hydrochloric acid solution. *Journal of colloid and interface science*, *502*, 134-145.

Koraee, H., Eskandari, H., & Danaee, I. (2019). Thermodynamic and Kinetic Investigations of Corrosion Inhibition Behavior of 2-MBT on Steel at a pH of 8. *Iranian Journal of Oil and Gas Science and Technology*, *8*(3), 101-112.

Ma, L., Li, W., Zhu, S., Wang, L., & Guan, S. (2021). Corrosion inhibition of Schiff bases for Mg-Zn-Y-Nd alloy in normal saline: Experimental and theoretical investigations. *Corrosion Science*, *184*, 109268.

Ma'rufah, L., Hanapi, A., Ningsih, R., & Fasya, A. G. (2021). Synthesis of Schiff Base Compounds from Vanillin and p-Aminoacetophenone Using Lime Juice as a Natural Acid Catalyst and Their Utilization as Corrosion Inhibitors. International Conference on Engineering, Technology and Social Science (ICONETOS 2020),

Minjibir, S. A., & Ladan, M. (2023). Corrosion Inhibition Potential of Prosopis Juliflora Leaves Extract on Mild Steel in H2SO4 Solutions. *Advanced Journal of Chemistry Section A*, *6*(3), 311-323.

Muhammad, A. A., Thomas, N. A., AbubakarMinjibir, S., Shehu, N. U., & Iorhuna, F. (2024). Exploring the Inhibition Potential of Carbamodithionic acid on Fe (111) Surface: A Theoretical Study. *Journal of Engineering in Industerial Research*, *4*, 201-210.

Musa, H., Bishir, U., Adamu, I. M., & Bashir, I. M. (2020). Effect of Aniline as Corrosion inhibitor on the Corrosion of Aluminium in Hydrochloric acid solution. *Res. J. Chem. Environ*, *24*(2).

Nyijime, T. A., Chahul, H. F., Ayuba, A., & Iorhuna, F. (2023). Theoretical investigations on thiadiazole derivatives as corrosion inhibitors on mild steel. *Adv. J. Chem. A*, *6*(2), 141-154.

Olasehinde, E. F., Olusegun, S., Adesina, A., Omogbehin, S., & Momoh, Y. H. (2012). Inhibitory action of Nicotiana tabacum extracts on the corrosion of mild steel in HCl: adsorption and thermodynamics study.

Omotosho, O. (2016). Inhibition evaluation of chemical and plant extracts on the corrosion of metallic alloys in acidic environment. *An Unpublished PhD. Thesis, Covenant University of Nigeria*.

Oshomogho, F. O., Akhihiero, T. E., Edokpayi, O., & Ossai, J. E. (2020). Green corrosion inhibition of mild steel using Prunus Dulcis seeds extract in an acidic medium. *Global Journal of Pure and Applied Sciences*, *26*(2), 171-178.

Pankaj, G., & Gargi, J. (2014). Corrosion inhibition by Aloe barbadensis (aloe vera) extract as green inhibitor for mild steel in HNO3. *Int. J. Sci. Res. Rev*, *3*(4), 72-83.

Ravari, F. B., & Dadgarinezhad, A. (2012). New Synthesized Schiff base as Inhibitor of Mild Steel Corrosion in Acid Medium. *Gazi University Journal of Science*, *25*(4), 835-842.

Selatnia, I., Sid, A., Benahmed, M., Dammene debbih, O., Ozturk, T., & Gherraf, N. (2018). Synthesis and characterization of a bis-pyrazoline derivative as corrosion inhibitor for A283 carbon steel in 1M HCl: electrochemical, surface, DFT and MD simulation studies. *Protection of Metals and Physical Chemistry of Surfaces*, *54*, 1182-1193.

Shehu, U., & Usman, B. (2023). Corrosion Inhibition of Iron Using Silicate Base Molecules: A Computational Study. *Advanced Journal of Chemistry, Section A*, *6*, 334.

Shkoor, M., Jalab, R., Khaled, M., Shawkat, T. S., Korashy, H. M., Saad, M., Su, H.-L., & Bani-Yaseen, A. D. (2023). Experimental and theoretical investigations of the effect of bis-phenylurea-based aliphatic amine derivative as an efficient green corrosion inhibitor for carbon steel in HCl solution. *Heliyon*, *9*(10).

Siaka, A., Eddy, N., Idris, S., & Magaji, L. (2014). Ampicillin potentials as Corrosion Inhibitor: Fukui function calculations using B3-YLP exchange correlation. *Nigerian Journal of Chemical Research*, *19*, 12-25.

Siaka, A. A., Eddy, N., Idris, S., Magaji, L., Garba, Z., & Shabanda, I. (2013). Quantum Chemical Studies of corrosion inhibition and adsorption potentials of Amoxicillin on mild steel in HCl solution. *International journal of modern Chemistry*, *4*(1), 1-10.

Verma, D. K., & Khan, F. (2016). Green approach to corrosion inhibition of mild steel in hydrochloric acid medium using extract of spirogyra algae. *Green chemistry letters and reviews*, *9*(1), 52-60.

Yaro, A. S., Khadom, A. A., & Wael, R. K. (2013). Apricot juice as green corrosion inhibitor of mild steel in phosphoric acid. *Alexandria Engineering Journal*, *52*(1), 129-135.